Supporting Information

Influence of A-site Cations on Germanium Iodates as Mid-IR Nonlinear Optical Materials: $A_2Ge(IO_3)_6$ (A = Li , K, Rb and Cs) and $BaGe(IO_3)_6 \cdot H_2O$

Hongming Liu,[a] Xingxing Jiang,[b] Xiaoxiao Wang,[a] Lei Yang,[b] Zheshuai Lin,[,b] Zhanggui Hu,[b] Xianggao Meng,[c] Xingguo Chen,[*,a] Jingui Qin[a]*

[a] Hubei Key Laboratory on Organic and Polymeric Opto-electronic Materials, College of Chemistry and Molecular Sciences, Wuhan University, Wuhan 430072, China. Email: xgchen@whu.edu.cn

[b] Beijing Center for Crystal R&D, Technical Institute of Physics and Chemistry, Chinese Academy of Sciences, Beijing 100190, China. Email: zslin@mail.ipc.ac.cn

[c] College of Chemistry, Central China Normal University, Wuhan 430079, China.

Figure S15 the electron structure along the highly symmetry path in the Brillouin zones in $Li_2Ge(IO_3)_6$ and $BaGe(IO_3)_6•H_2O$.

Figure S16 the refractive index dispersion of $Li_2Ge(IO_3)_6$ and $BaGe(IO_3)_6•H_2O$

Table S1. Selected bond lengths (Å) for $Li_2Ge(IO_3)_6$

Bond	Lengths (Å)	Bond	Lengths (Å)
Ge(1)-O(1)#2	2.003(13)	I(1)-O(3)	1.776(10)
Ge(1)-O(1)#3	2.003(13)	I(1)-O(2)	1.778(10)
Ge(1)-O(1)#4	2.003(13)	I(1)-O(1)	1.857(12)
Ge(1)-O(1)#5	2.012(14)	Li(1)-O(2) X 3	2.111(19)
Ge(1)-O(1)	2.012(14)	Li(1)-O(3) X 3	2.208(19)
Ge(1)-O(1)#6	2.012(14)		

Table S2. Selected bond lengths (Å) for $A_2Ge(IO_3)_6$ (A=K, Rb and Cs)

Bond	$K_2Ge(IO_3)_6$	$Rb_2Ge(IO_3)_6$	$Cs_2Ge(IO_3)_6$
I(1)-O(3)	1.793(4)	1.788(3)	1.787(4)
I(1)-O(2)	1.800(4)	1.799(3)	1.790(4)
I(1)-O(1)	1.881(4)	1.872(3)	1.869(4)
Ge(1)-O(1)#2	1.881(4)	1.889(3)	1.886(4)
Ge(1)-O(1)#6	1.881(4)	1.889(3)	1.886(4)
Ge(1)-O(1)#7	1.881(4)	1.889(3)	1.886(4)
Ge(1)-O(1)#8	1.881(4)	1.889(3)	1.886(4)
Ge(1)-O(1)	1.882(4)	1.889(3)	1.886(4)
Ge(1)-O(1)#9	1.882(4)	1.889(2)	1.886(4)
A(1)-O(1) X 3	2.966(4)	2.897(3)	3.057(4)
A(1)-O(2) X 3	2.776(4)	3.047(3)	3.162(4)
A(1)-O(3) X 3	2.971(4)	3.054(3)	3.170(4)

Table S3. Selected bond lengths (Å) for $BaGe(IO_3)_6 \cdot H_2O$

Bond	Lengths (Å)	Bond	Lengths (Å)
Ge(1)-O(4)	1.872(6)	Ba(1)-O(8)	2.611(10)
Ge(1)-O(4)#4	1.872(6)	Ba(1)-O(6)#1	2.753(6)
Ge(1)-O(4)#5	1.872(6)	Ba(1)-O(6)#2	2.753(6)
Ge(1)-O(2)#4	1.884(6)	Ba(1)-O(6)#3	2.753(6)
Ge(1)-O(2)	1.884(6)	Ba(1)-O(1)	2.994(6)
Ge(1)-O(2)#5	1.884(5)	Ba(1)-O(1)#4	2.994(6)
I(1)-O(3)	1.783(6)	Ba(1)-O(1)#5	2.994(6)
I(1)-O(1)	1.794(5)	Ba(1)-O(3)#6	3.012(6)
I(1)-O(2)	1.860(5)	Ba(1)-O(3)#7	3.012(6)
I(2)-O(5)	1.784(6)	Ba(1)-O(3)#8	3.012(6)
I(2)-O(6)	1.784(6)		
I(2)-O(4)	1.869(6)		

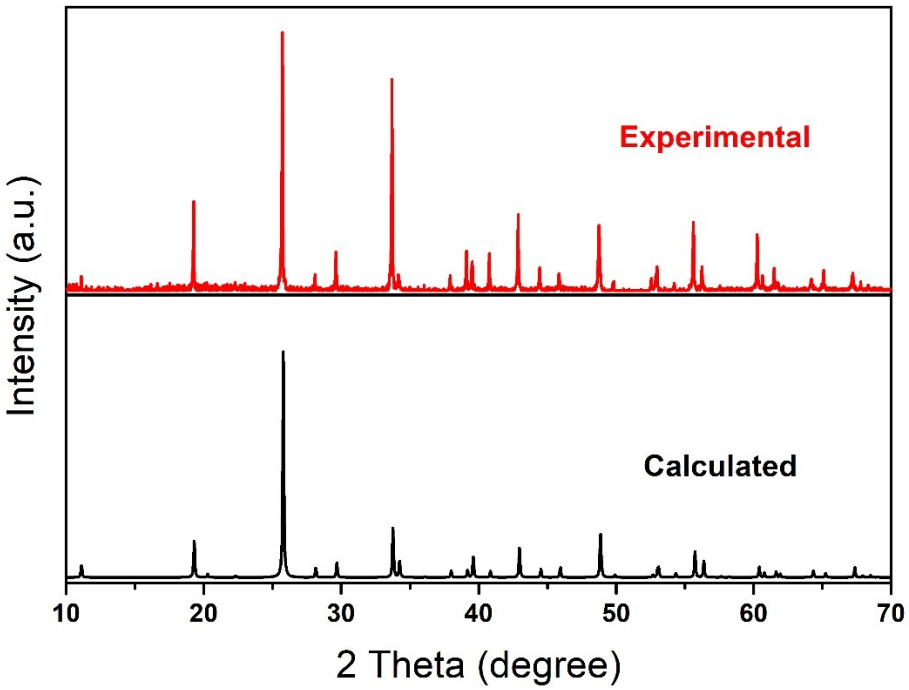

Figure S1. Simulated and measured powder X-ray diffraction patterns of $Li_2Ge(IO_3)_6$

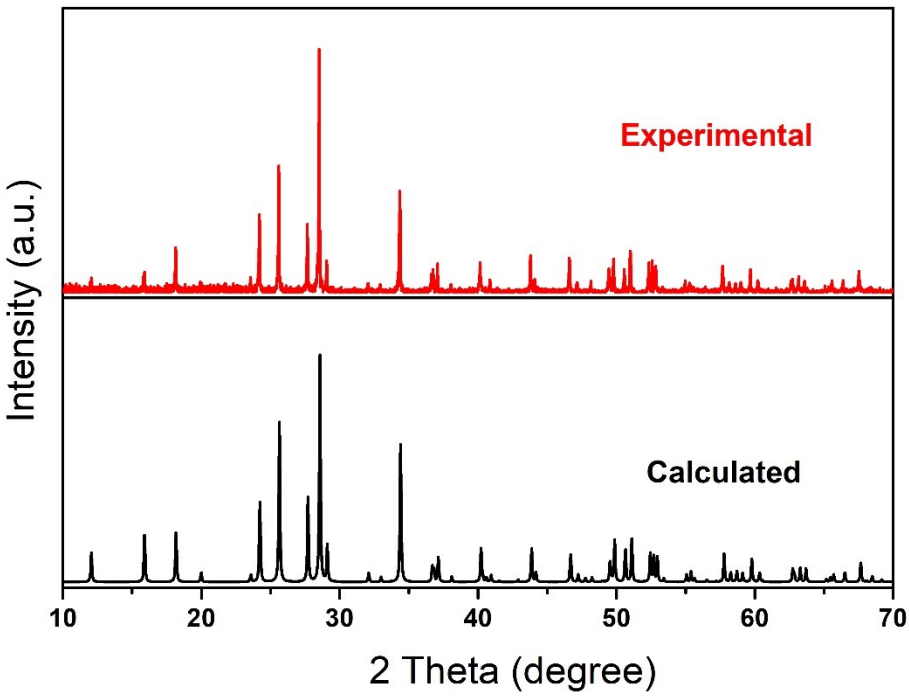

Figure S2. Simulated and measured powder X-ray diffraction patterns of $K_2Ge(IO_3)_6$

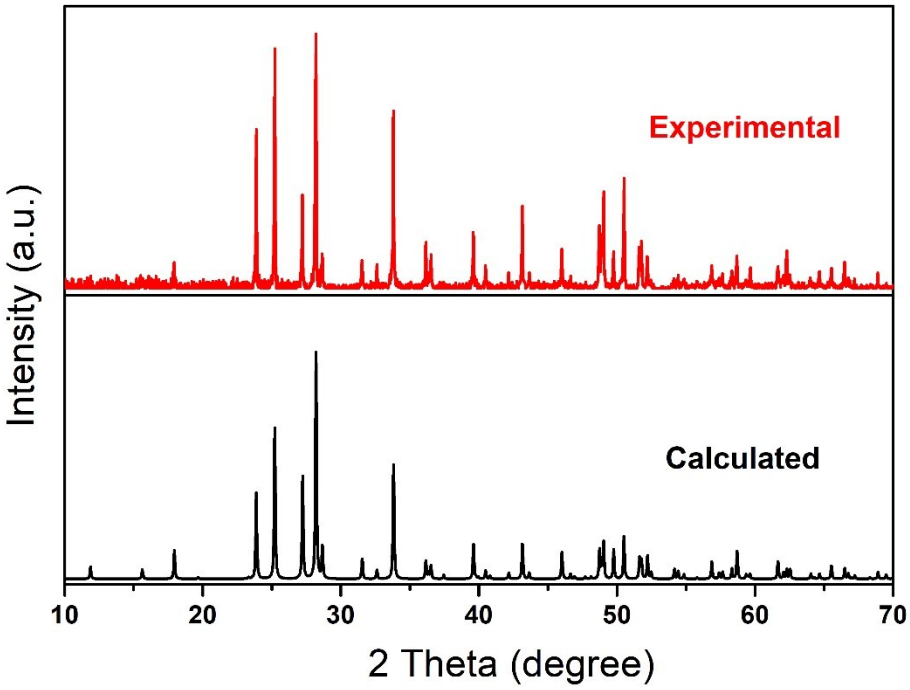

Figure S3. Simulated and measured powder X-ray diffraction patterns of $Rb_2Ge(IO_3)_6$

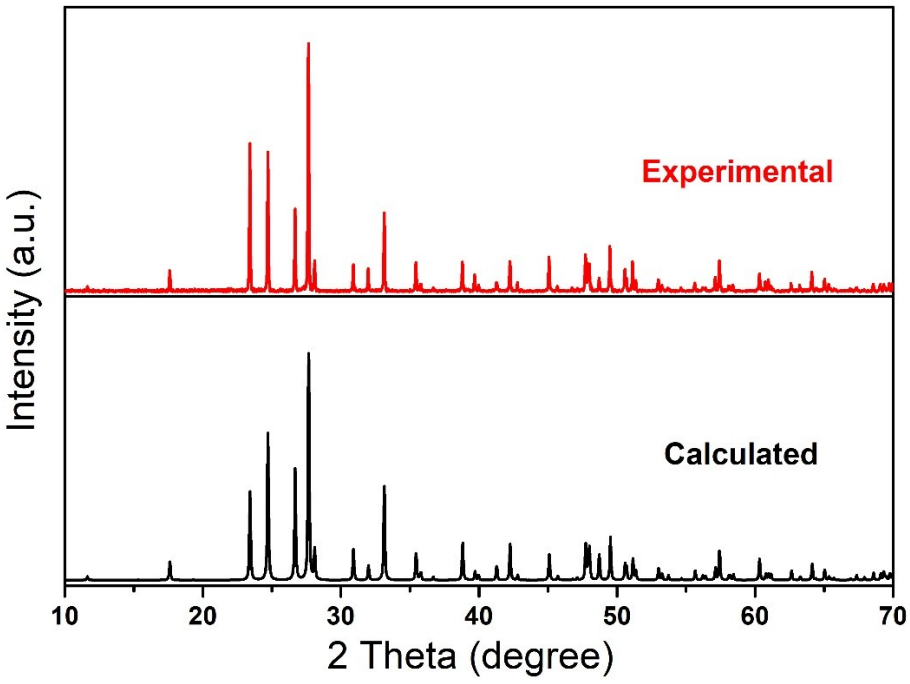

Figure S4. Simulated and measured powder X-ray diffraction patterns of $Cs_2Ge(IO_3)_6$

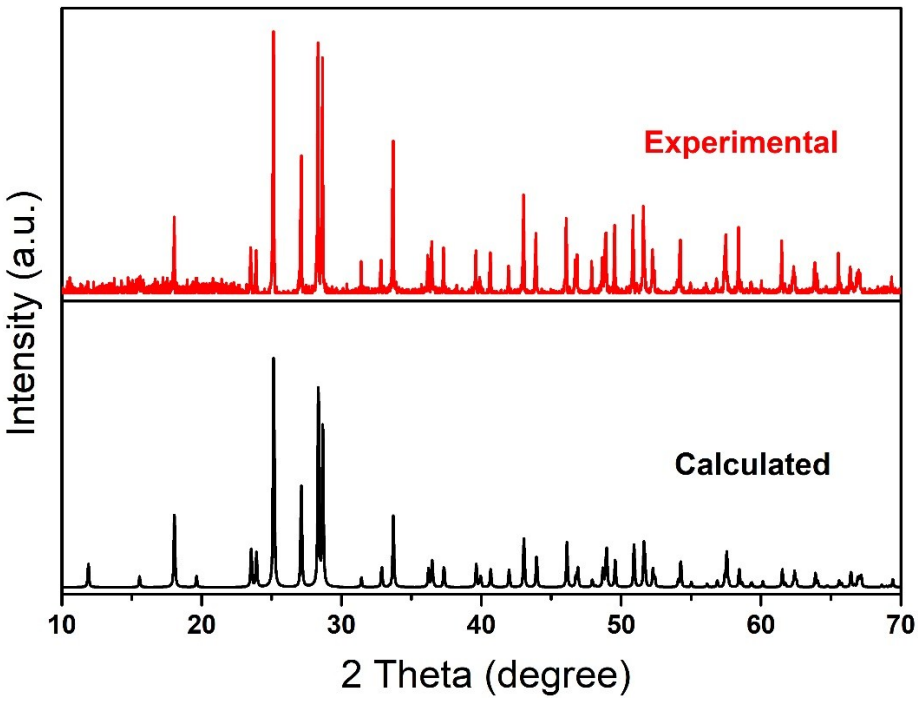

Figure S5. Simulated and measured powder X-ray diffraction patterns of $BaGe(IO_3)_6 \cdot H_2O$

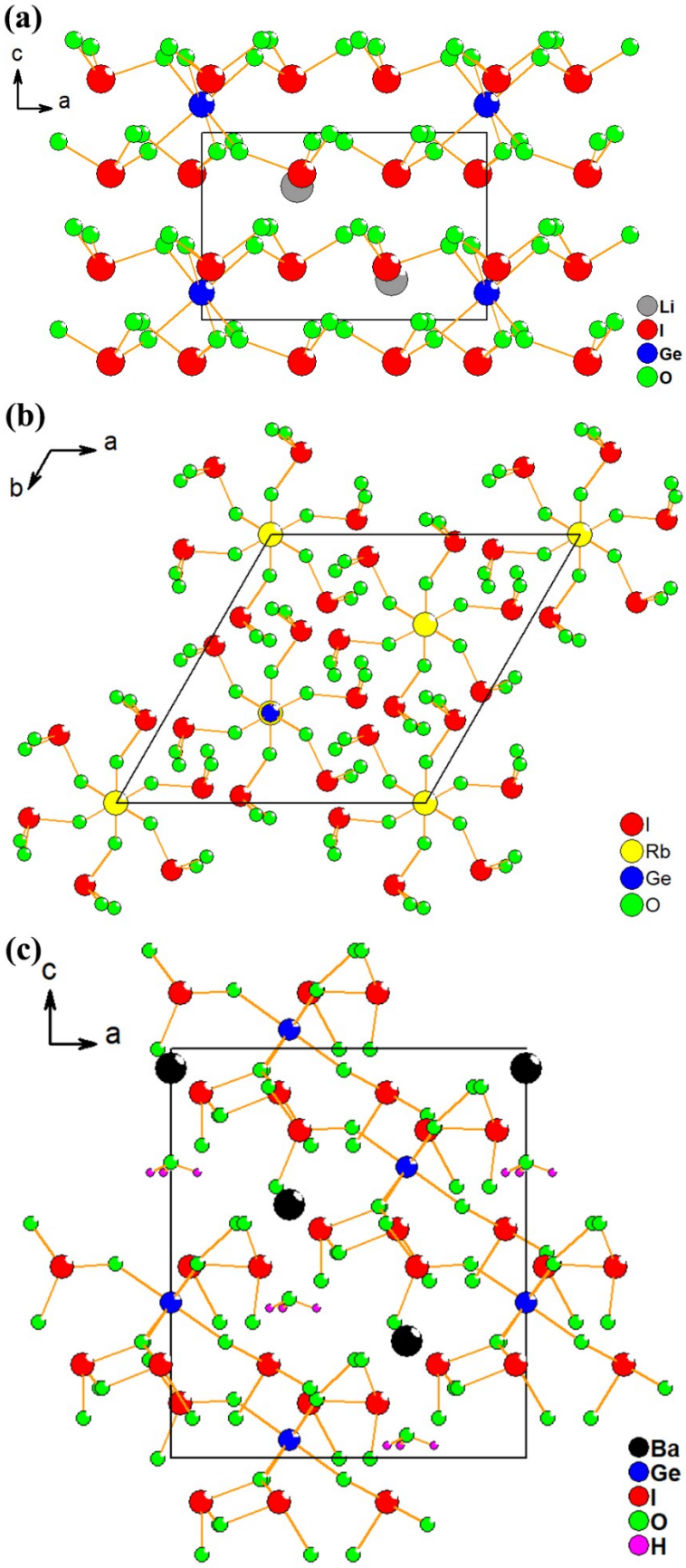

Figure S6. The structures of a) $Li_2Ge(IO_3)_6$, b) $Rb_2Ge(IO_3)_6$ and c) $BaGe(IO_3)_6 \cdot H_2O$

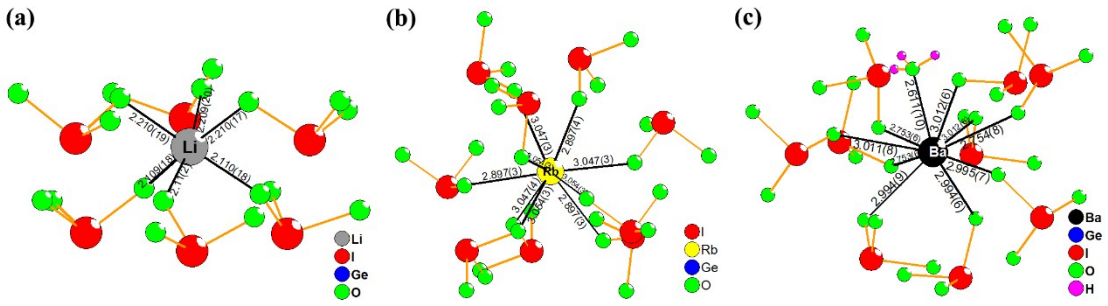

Figure S7. The coordination environments of Li^{+}, Rb^{+} and Ba^{2+} cations in a) $Li_2Ge(IO_3)_6$, b) $Rb_2Ge(IO_3)_6$ and c) $BaGe(IO_3)_6 \cdot H_2O$

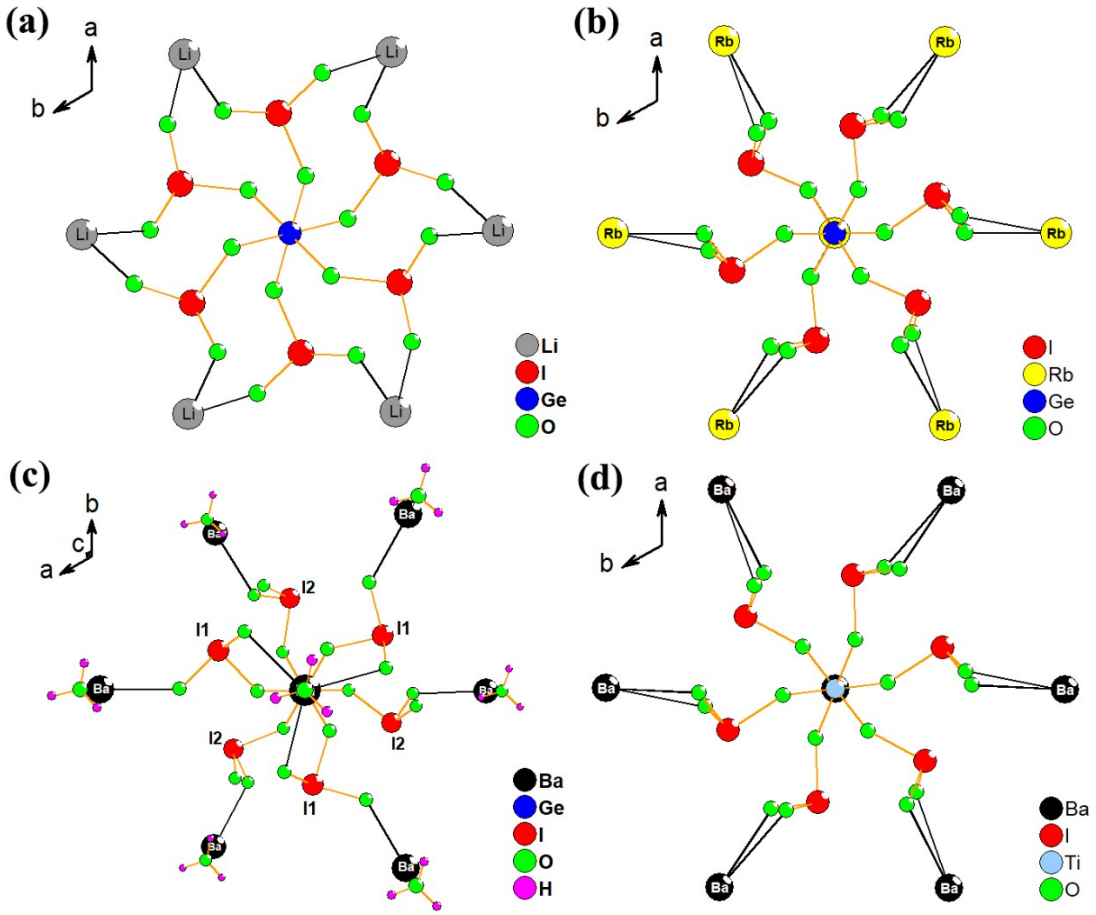

Figure S8. The coordinated environments of IO_3 groups in a) $Li_2Ge(IO_3)_6$, b) $Rb_2Ge(IO_3)_6$, c) $BaGe(IO_3)_6 \cdot H_2O$ and d) $BaTi(IO_3)_6$ [1].

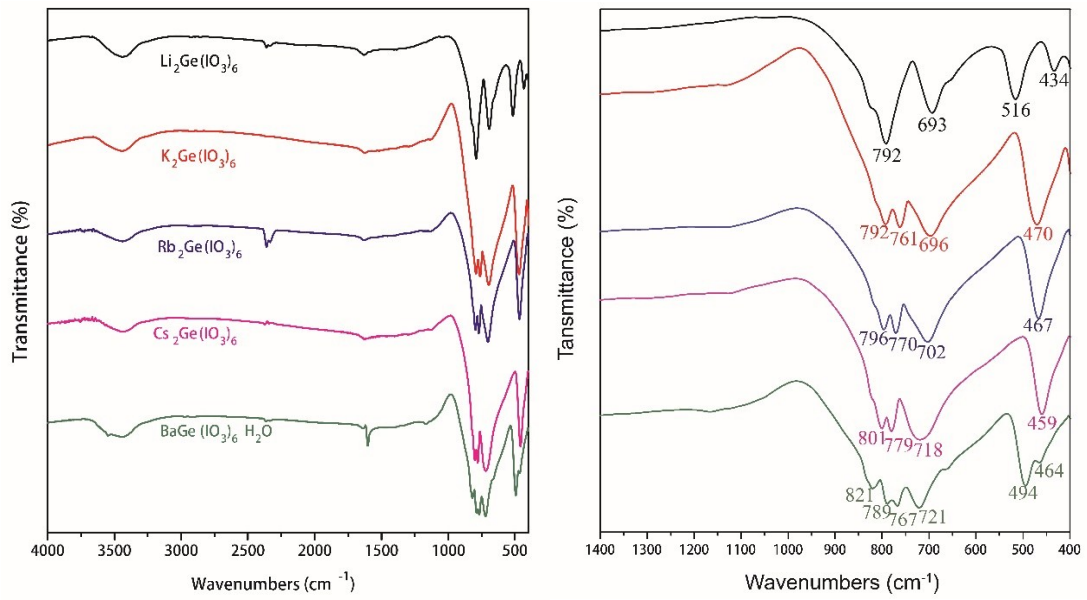

Figure S9. Infrared spectra of $A_2Ge(IO_3)_6$ (A=Li, K, Rb and Cs) and $BaGe(IO_3)_6 \bullet H_2O$

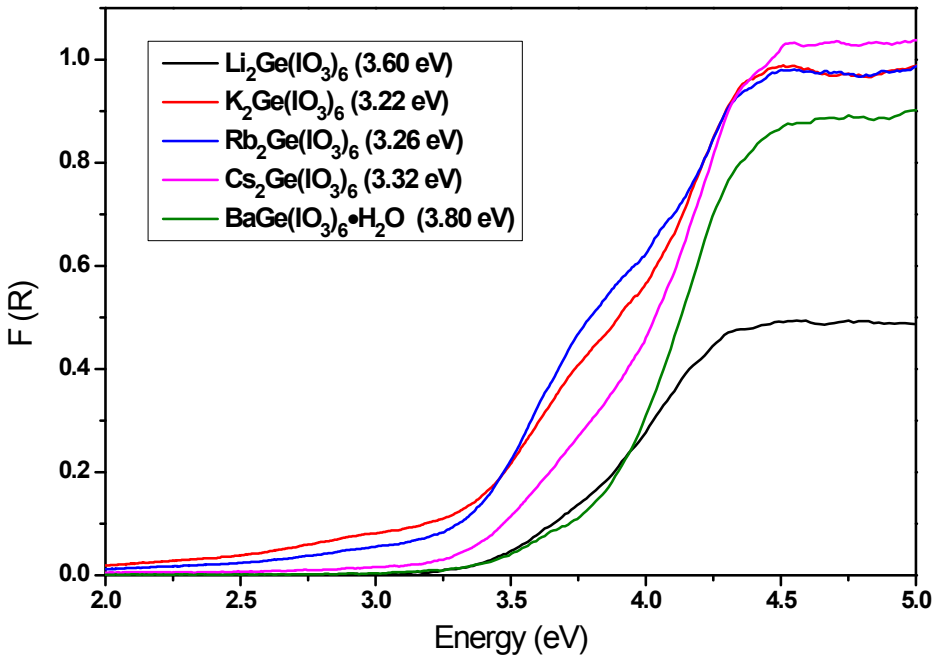

Figure S10. UV-Vis diffuse reflectance spectra of $A_2Ge(IO_3)_6$ (A=Li, K, Rb and Cs) and $BaGe(IO_3)_6 \bullet H_2O$

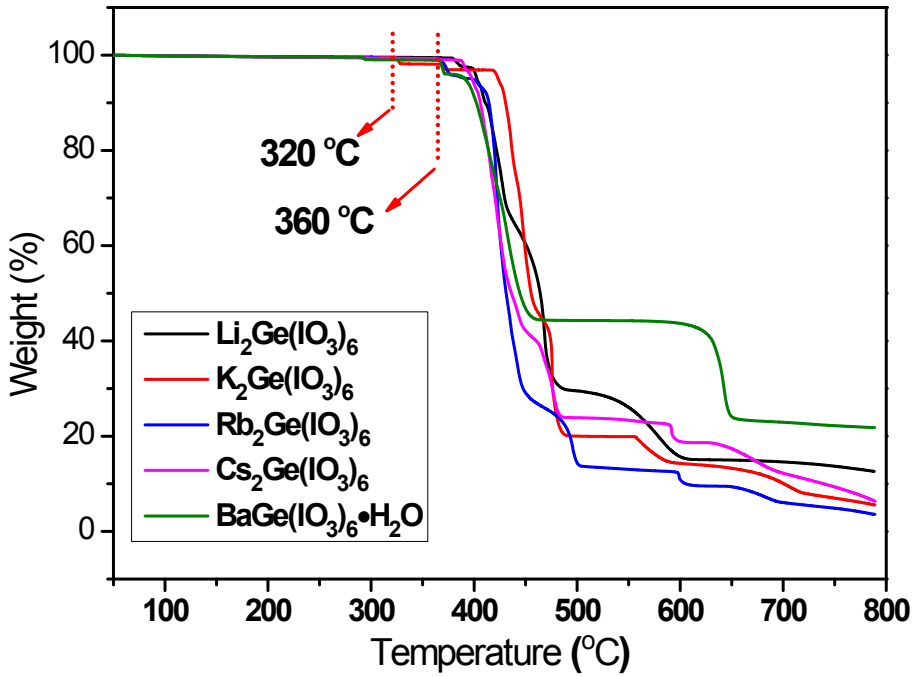

Figure S11. The TGA curves of $A_2Ge(IO_3)_6$ (A=Li, K, Rb and Cs) and $BaGe(IO_3)_6 \cdot H_2O$

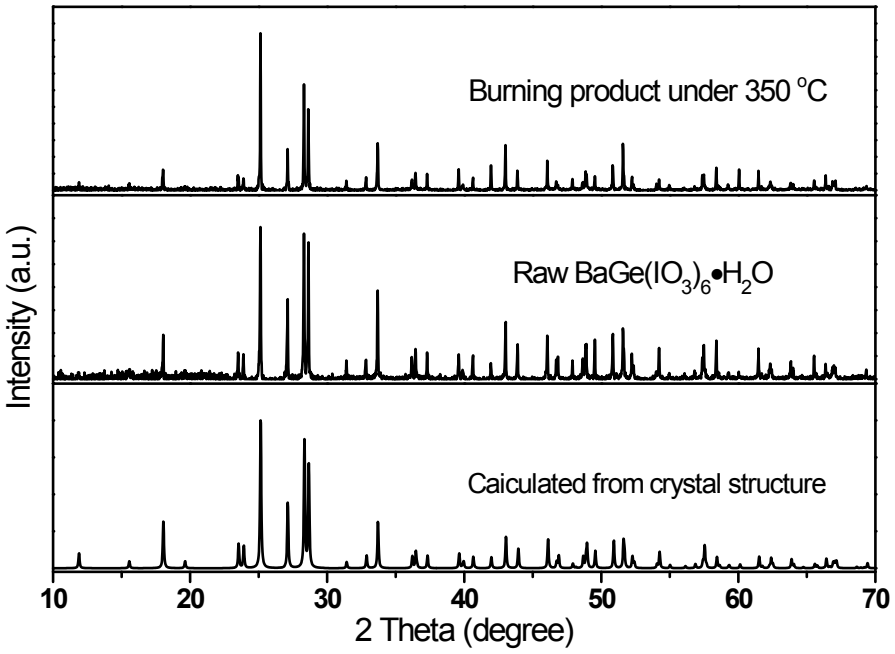

Figure S12. The XRD patterns of the burning product under 350 °C of $BaGe(IO_3)_6 \cdot H_2O$

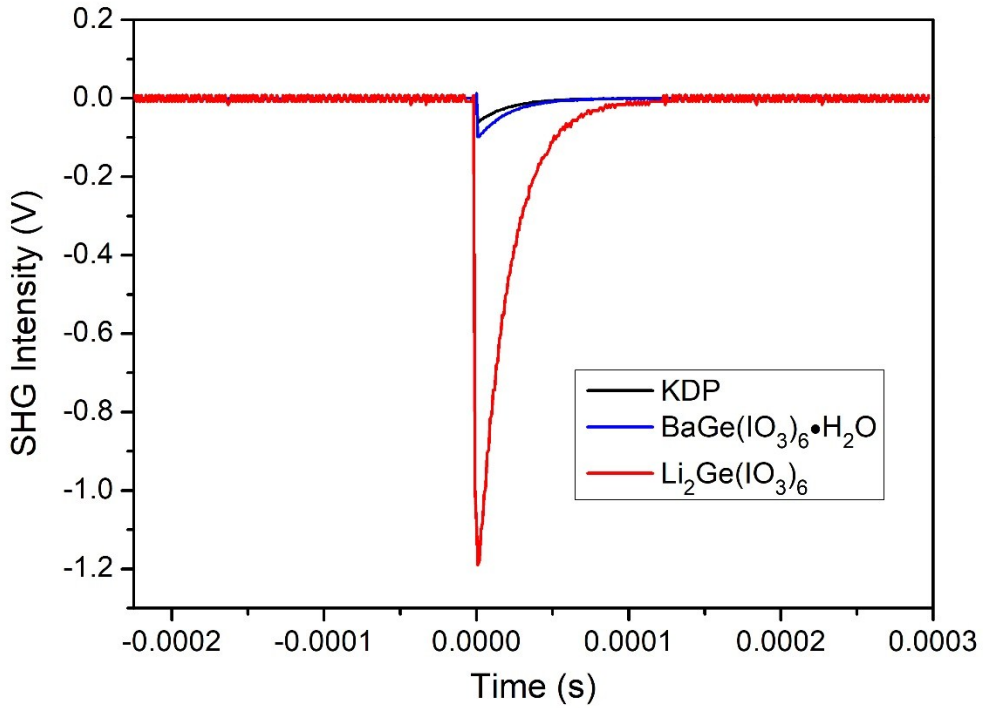

Figure S13. Oscilloscope traces of the SHG signals for KDP, $BaGe(IO_3)_6 \cdot H_2O$ and $Li_2Ge(IO_3)_6$ at the powder size of 300–400 μm under 1064 nm laser radiation

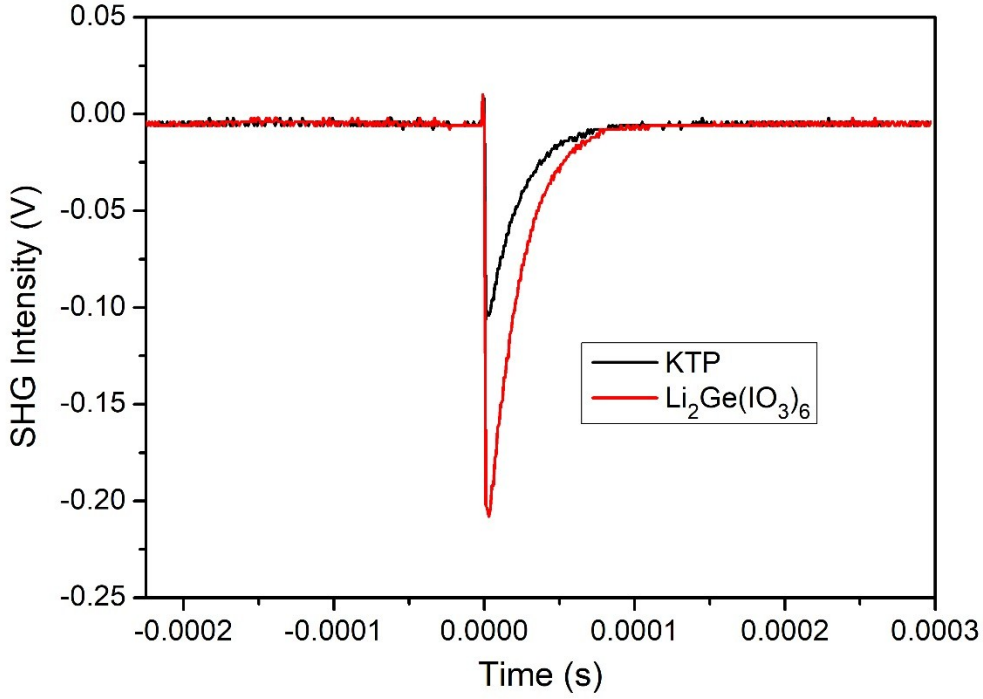

Figure S14. Oscilloscope traces of the SHG signals for KTP and $Li_2Ge(IO_3)_6$ at the powder size of 300–400 μm under 1950 nm laser radiation

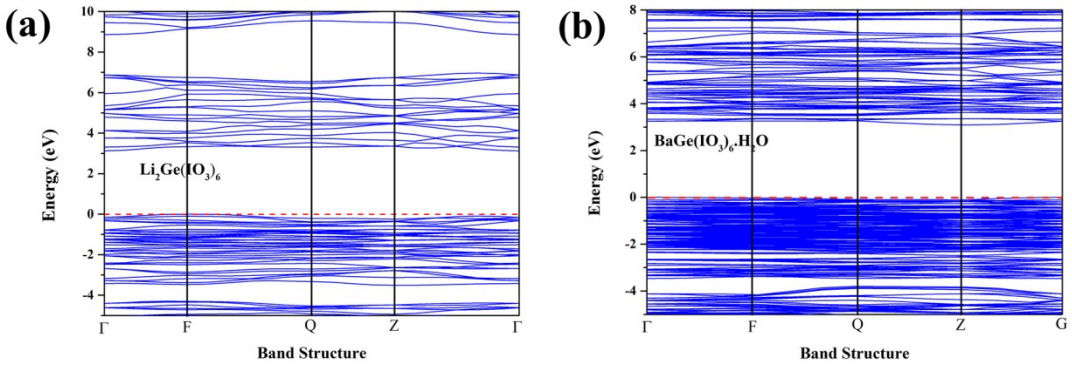

Figure S15 the electron structure along the highly symmetry path in the Brillouin zones in $Li_2Ge(IO_3)_6$(a) and $BaGe(IO_3)_6$•H_2O(b).

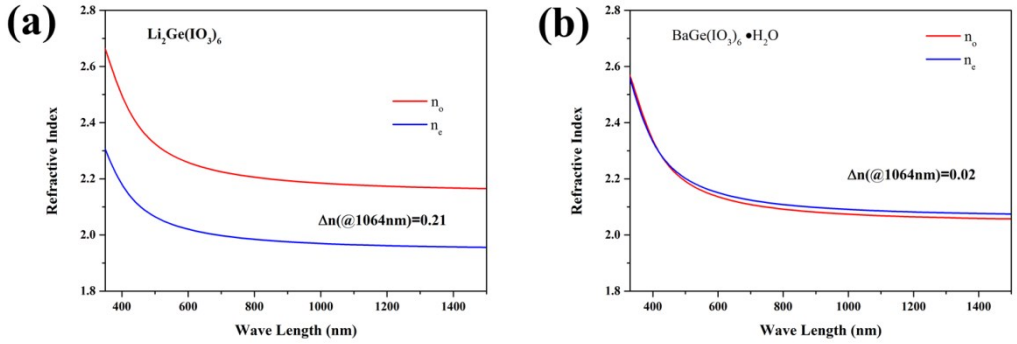

Figure S16 the refractive index dispersion of $Li_2Ge(IO_3)_6$(a) and $BaGe(IO_3)_6$•H_2O(b)

Reference

[1] K. M. Ok and P. S. Halasyamani, *Inorg. Chem.*, 2005, **44**(7), 2263-2271.